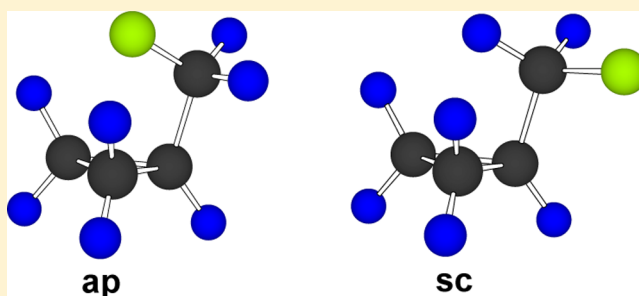


Microwave Spectrum, Conformational Composition, and Dipole Moment of (Fluoromethyl)cyclopropane ($C_3H_5CH_2F$)Svein Samdal,[†] Harald Møllendal,^{*,†} and Jean-Claude Guillemin[‡][†]Centre for Theoretical and Computational Chemistry (CTCC), Department of Chemistry, University of Oslo, P.O. Box 1033 Blindern, NO-0315 Oslo, Norway[‡]Institut des Sciences Chimiques de Rennes, École Nationale Supérieure de Chimie de Rennes, CNRS, UMR 6226, 11 Allée de Beaulieu, CS 50837, 35708 Rennes Cedex 7, France

S Supporting Information

ABSTRACT: The microwave spectrum of (fluoromethyl)-cyclopropane, $C_3H_5CH_2F$, has been investigated in the whole 12–75.6 GHz spectral range. Many measurements were also performed in the 75.6–120 GHz region. The spectra of two conformers were assigned. The H–C–C–F chain of atoms is antiperiplanar in the conformer denoted **ap** and synclinal in the **sc** rotamer. The **sc** conformer has a lower energy than **ap**. The internal energy difference was determined to be $E_{ap} - E_{sc} = 1.7(8)$ kJ/mol from relative intensity measurements. The spectra of the ground vibrational state and seven vibrationally excited states belonging to two different normal modes were assigned for **sc**. The frequencies of these two modes were determined by relative intensity measurements. The dipole moment of this conformer was determined to be $\mu_a = 5.520(17)$, $\mu_b = 3.475(29)$, $\mu_c = 0.35(13)$, and $\mu_{TOT} = 6.532(40) \times 10^{-30}$ C m [1.958(12) D]. The spectrum of the ground vibrational state was assigned for **ap**. The microwave work was supported by quantum chemical calculations at the CCSD/cc-pVQZ, MP2/cc-pVTZ, and B3LYP/cc-pVTZ levels of theory.



■ INTRODUCTION

Conformational and structural studies of methylcyclopropane derivatives ($C_3H_5CH_2X$) have received considerable attention in the past. Microwave (MW), infrared (IR), and Raman spectroscopic studies, often augmented by quantum chemical calculations, have been reported for a number of them including $X = F$,^{1–4} Cl ,^{2,5–8} Br ,^{2,6,8,9} I ,^{2,10} OH ,¹¹ SH ,¹² SeH ,¹³ NH_2 ,¹⁴ PH_2 ,¹⁵ CH_3 ,¹⁶ SiH_3 ,^{17–20} SiF_3 ,^{17,21,22} $C\equiv N$,^{23,24} $C\equiv C-H$,^{25,26} and $N\equiv C$.²⁷

The orientation of the H–C–C–X chain of atoms can conveniently be used to characterize the conformers of the $C_3H_5CH_2X$ compounds. Two rotamers generally exist for these molecules. In one of them, this link of atoms is *antiperiplanar* and forms a dihedral angle of exactly 180° . This conformer has a symmetry plane bisecting the cyclopropyl ring. In the second rotamer, the H–C–C–X chain has a *synclinal* orientation and has a dihedral angle of about 60° . Obsolete nomenclature, “*cis*” and “*gauche*” for antiperiplanar and synclinal forms, respectively, is often encountered.

It has generally been found in these comprehensive studies that the synclinal H–C–C–X form predominates with one exception, namely, $C_3H_5CH_2C\equiv CH$, where the antiperiplanar form is 0.77(36) kJ/mol lower in energy.²⁵ It has also been found that the synclinal form becomes increasingly more stable as the size of the substituent X increases. Steric effects therefore appear to be important for the conformational preferences of these molecules. The *gauche* effect²⁸ should also favor the

synclinal orientation, especially when X is electronegative. Intramolecular hydrogen bonding with the pseudo- π electrons²⁹ of the cyclopropyl ring is another interaction that will stabilize the synclinal forms in some of these compounds, for example, $X = OH$,¹¹ SH ,¹² SeH ,¹³ NH_2 ,¹⁴ and PH_2 .¹⁵ Further examples are discussed in a review.³⁰

The antiperiplanar and synclinal forms of the title compound, $C_3H_5CH_2F$, are denoted **ap** and **sc** and depicted with atom numbering in Figure 1. This compound has been investigated by a variety of experimental and theoretical methods. Stølevik and Bakken² using molecular mechanics calculations concluded that **ap** is lower in energy than **sc** by 2.2 kJ/mol. Saebo and Kavana³ found from their MP4(SDQ)/6-311G** computations that the opposite conformational preference exists, with **sc** 0.8 kJ/mol lower in energy than **ap**. Durig et al.^{1,4} determined an energy difference of 3.13(31) kJ/mol favoring **sc** from a variable temperature infrared study of this compound dissolved in xenon.

No MW studies of $C_3H_5CH_2F$ have been reported. The conformational composition in the gas may differ from that of the xenon solution. MW spectroscopy is an ideal method to study conformational equilibria due to its superior accuracy and resolution. Another advantage is that accurate energy

Received: January 28, 2014

Revised: February 21, 2014

Published: February 27, 2014



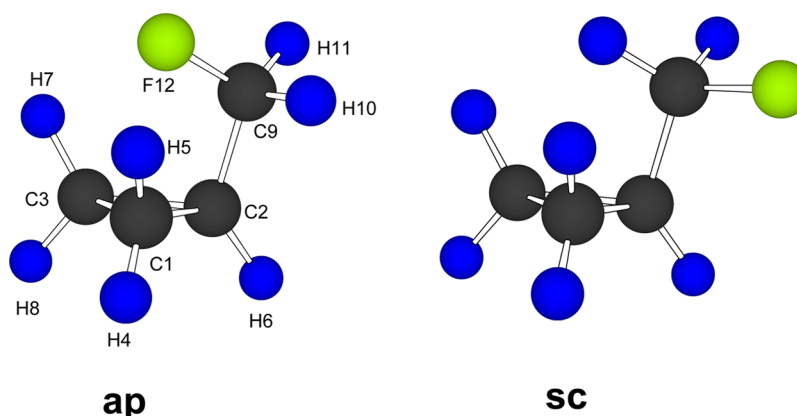


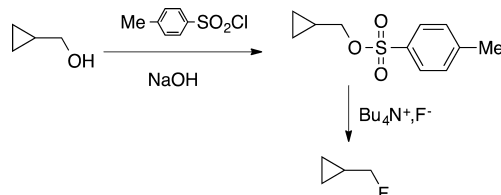
Figure 1. Models of the H6–C2–C9–F12 *antiperiplanar* (**ap**) and *synclinal* (**sc**) conformers of (fluoromethyl)cyclopropane. **sc** was found to be 1.7(8) kJ/mol more stable than **ap** from relative intensity measurements.

differences can be obtained by this method. We have therefore undertaken the first MW investigation of (fluoromethyl)cyclopropane. The MW study has been augmented with quantum chemical calculations at a much higher level than previously.^{1,3,4} These computations were conducted with the purpose of obtaining information for use in assigning the MW spectrum and investigating properties of the potential-energy hypersurface.

EXPERIMENTAL SECTION

Synthesis of (Fluoromethyl)cyclopropane. (Fluoromethyl)cyclopropane³¹ has been synthesized according to Scheme 1 in a two-step sequence starting from the

Scheme 1



cyclopropanemethanol (see the Supporting Information for experimental procedures). This procedure was chosen instead of the reaction between cyclopropanemethanol and diethylaminosulfur trifluoride (DAST) in which fluorocyclobutane is formed as a byproduct. The advantage of the present approach (Scheme 1) is that no fluorocyclobutane is formed.

Spectroscopic Experiments. C₃H₅CH₂F is a colorless, volatile liquid at room temperature. The MW spectrum was recorded at room temperature, or with the cell cooled to about –30 °C using small portions of dry ice to cool the waveguide. The pressure was 5–10 Pa during the measurements. The MW spectrum was studied with Stark-modulation spectroscopy using the microwave spectrometer of the University of Oslo. Details of the construction and operation of this device have been given elsewhere.³² This spectrometer has a resolution of about 0.5 MHz and measures the frequency of isolated transitions with an estimated accuracy of ~0.10 MHz. The spectrum was investigated in the whole 12–75.6 GHz frequency interval. Many measurements were also performed in the 75.6–120 GHz region. Radio-frequency microwave double-resonance experiments (RFMWDR), similar to those of Wodarczyk and Wilson,³³ were also conducted to unambiguously assign

particular transitions, using the equipment described elsewhere.³⁴

RESULTS AND DISCUSSION

Quantum Chemical Methods. The present ab initio Møller–Plesset second-order perturbation calculations³⁵ (MP2), coupled cluster singles and doubles^{36–39} (CCSD), and density functional theory (DFT) calculations were performed employing the Gaussian 09⁴⁰ and Molpro program packages⁴¹ running on the Abel cluster in Oslo. Becke’s three-parameter hybrid functional employing the Lee, Yang, and Parr exchange-correlation functional (B3LYP)⁴² was employed in the DFT computations. Peterson and Dunning’s⁴³ correlation-consistent cc-pVTZ and cc-pVQZ basis sets, which are of triple- and quadruple- ζ quality, were used in the calculations.

Quantum Chemical Calculations. MP2/cc-pVTZ calculations of the optimized structures and dipole moments of **ap** and **sc** were first performed. All structural parameters were varied freely in these calculations with no symmetry restrictions. The vibrational frequencies, Watson’s *S*-reduction quartic and sextic centrifugal distortion constants,⁴⁴ the vibration–rotation interaction constants⁴⁵ (the α ’s), and the equilibrium and effective rotational constants were then calculated using the principal inertial axes coordinates of the optimized structures, which were kept fixed in the calculations, as pointed out by McKean et al.⁴⁶ The results of these calculations are found in Tables 1S and 2S of the Supporting Information. Centrifugal distortion constants are repeated in the last columns of Tables 2 and 5 for comparison with their experimental counterparts.

It is seen from Tables 1S and 2S (Supporting Information) that no imaginary harmonic normal vibrations were obtained for any of the two forms, which is an indication that **ap** and **sc** are indeed minima on the potential-energy hypersurface. **ap** was found to have the expected symmetry plane consisting of the H6–C2–C9–F12 link of atoms. The important H6–C2–C9–F12 dihedral angle was found to be 65.3° in **sc** and exactly 180° in **ap**. The MP2 energy difference corrected for the zero-point vibrational effect is 2.54 kJ/mol, with **sc** as the lower-energy rotamer, whereas the electronic MP2 energy difference is 2.34 kJ/mol.

The B3LYP/cc-pVTZ and MP2/cc-pVTZ potential functions for rotation about the C2–C9 bond were calculated using the scan option of Gaussian 09 in order to compare an ab initio and a DFT method. The H6–C2–C9–F12 dihedral angle was

Table 1. CCSD/cc-pVQZ Structures, Energy Difference, and Dipole Moments of the **ap** and **sc** Conformers of C₃H₅CH₂F

conformer:	ap	sc	conformer:	ap	sc
Bond Distance (pm)			Angle (deg)		
C1–C2	149.9	150.0	H10–C9–F12	107.4	107.2
C1–C3	150.7	150.2	H11–C9–F12	107.4	107.6
C1–H4	107.9	107.8	Dihedral Angle (deg)		
C1–H5	107.9	108.0	H4–C1–C2–H6	1.0	1.1
C2–C3	149.9	150.4	H4–C1–C2–C9	–142.1	–144.4
C2–H6	108.2	108.0	H5–C1–C2–H6	146.1	145.0
C2–C9	150.1	149.2	H5–C1–C2–C9	3.0	–0.6
C3–H7	107.9	108.0	H4–C1–C3–H7	144.9	144.7
C3–H8	107.9	107.8	H4–C1–C3–H8	0.0	–0.3
C9–H10	109.0	109.0	H5–C1–C3–H7	0.0	–0.4
C9–H11	109.0	109.1	H5–C1–C3–H8	–144.9	–145.5
C9–F12	138.4	138.5	H6–C2–C3–H7	–146.1	–145.1
Angle (deg)			H6–C2–C3–H8	–1.0	–1.1
C2–C1–H4	118.0	117.9	C9–C2–C3–H7	–3.0	–1.2
C2–C1–H5	117.3	117.3	C9–C2–C3–H8	142.1	142.8
C3–C1–H4	118.2	118.1	C1–C2–C9–H10	83.5	–159.5
C3–C1–H5	116.9	117.9	C1–C2–C9–H11	–154.7	–38.0
H4–C1–H5	115.4	114.8	C1–C2–C9–F12	–35.6	81.2
C1–C2–H6	116.8	117.0	C3–C2–C9–H10	154.7	–90.2
C1–C2–C9	120.2	118.8	C3–C2–C9–H11	–83.5	31.3
C3–C2–H6	116.8	116.9	C3–C2–C9–F12	35.6	150.4
C3–C2–C9	120.2	118.0	H6–C2–C9–H10	–60.9	54.3
H6–C2–C9	112.9	115.1	H6–C2–C9–H11	60.9	175.9
C1–C3–H7	116.9	117.8	H6–C2–C9–F12	180.0	–65.0
C1–C3–H8	118.2	118.3	Electronic Energy Difference ^a (kJ/mol)		
C2–C3–H7	117.3	117.7		2.94	0.0
C2–C3–H8	118.0	117.8	Dipole Moment ^b (10 ^{–30} C m)		
H7–C3–H8	115.4	114.6	μ_a	2.54	5.56
C2–C9–H10	111.2	111.6	μ_b	5.32	3.42
C2–C9–H11	111.2	110.5	μ_c	0.0 ^c	0.48
C2–C9–F12	110.5	110.7	μ_{tot}	5.89	6.54
H10–C9–H11	109.1	109.0			

^aThe CCSD/cc-pVQZ electronic energy of the **sc** conformer: –672337.45 kJ/mol. The energy of the **ap** form is 2.94 kJ/mol higher than the energy of the **sc** rotamer. ^b1 D = 3.33564 × 10^{–30} C m. ^cFor symmetry reasons.

stepped in 10° intervals in these calculations. The functions are drawn in Figure 2, MP2 (black) and B3LYP (red). The MP2 curve has minima at 65.3° (**sc**) and exactly 180° (**ap**). The MP2 electronic energy difference between these two conformers are 2.34 kJ/mol favoring **sc**. The maxima of the MP2 graph are at exactly 0°, 19.65 kJ/mol above the **sc** minimum, and at 125.4°, 14.53 kJ/mol above the **sc** minimum. The B3LYP calculations yielded an energy difference of 2.65 kJ/mol between **ap** and **sc**. The two maxima at 0 and 125.5° have energies that are 16.86 and 12.84 kJ/mol higher than the B3LYP energy of **sc**. The agreement between the two methods is quite good.

Finally, comprehensive CCSD/cc-pVQZ calculations of optimized structures, dipole moments, and electronic energies of **ap** and **sc** were performed using the MP2 structures in Tables 1S and 2S (Supporting Information) as starting points. **ap** was assumed to have a symmetry plane in these calculations to save computational time. Unfortunately, it is not possible to calculate centrifugal distortion constants at the CCSD level with our present computational resources.

The resulting CCSD structures are listed in Table 1. Further structural details are listed in Table 3S (**ap**) and 4S (**sc**) of the Supporting Information. The electronic energy difference and the dipole moments are included in Table 1. The rotational

constants obtained from the CCSD structures are shown together with their experimental equivalents in the last columns of Tables 2 and 5.

Some of the CCSD results warrant further comments. The CCSD electronic energy difference is 2.94 kJ/mol with **sc** as the lower-energy conformer, compared to the MP2 (2.34 kJ/mol) and B3LYP (2.65 kJ/mol).

The C–C bond lengths of the cyclopropyl ring vary between 150.0 and 150.7 pm (Table 1), compared to the equilibrium bond length in cyclopropane, which is 151.0077(77) pm.⁴⁷ The variation of the bond lengths of the cyclopropyl ring is interesting. The C1–C3 bond length, which is opposite to the fluoromethyl substituent, is slightly longer by 0.4–0.7 pm than the adjacent C1–C2 and C2–C3 bond lengths. This asymmetry is typical for substituted cyclopropanes.⁴⁸ The C–F bond length is 138.4 pm in **ap** and 138.5 pm in **sc**, almost the same as the equilibrium C–F bond length in CH₃F, which is 138.3(1) pm.⁴⁹

Variations of corresponding bond angles of the two conformers are less than about 2°. Interestingly, the H6–C2–C9–F12 dihedral angle, which determines the conformational properties of this compound, is 65.0° in **sc**, 5° larger than the “canonical” 60°. This CCSD angle is similar to 65.3 and 64.9° found in the MP2 and B3LYP calculations, respectively.

Table 2. Spectroscopic Constants of the Ground Vibrational State of the *sc* Conformer and Their Theoretical Counterparts

	ground state ^a	theory ^b
<i>A</i> (MHz)	12745.9346(19)	12901.40
<i>B</i> (MHz)	3175.40028(50)	3198.43
<i>C</i> (MHz)	2858.34908(52)	2880.90
<i>D_J</i> (kHz)	1.29841(40)	1.28
<i>D_{JK}</i> (kHz)	−4.5535(39)	−4.26
<i>D_K</i> (kHz)	26.3440(23)	24.9
<i>d₁</i> (kHz)	−0.21559(13)	−0.205
<i>d₂</i> (kHz)	−0.012105(59)	−0.0113
<i>H_J</i> (Hz)	0.00261(10)	0.00109
<i>H_{JK}</i> (Hz)	−0.0352(20)	−0.0905
<i>H_{KJ}</i> (Hz)	0.0841(22)	0.458
<i>H_K</i> (Hz)	−0.1082(55)	−1.02
<i>h₁</i> (Hz)	0.00398(67)	−0.0000525
<i>h₂</i> (Hz)	0.000095(46)	−0.000198
<i>h₃</i> (Hz)	0.000027(11)	−0.00000169
rms ^c	1.274	
<i>N</i> ^d	1130	

^aS-reduction *I*^r-representation.⁴⁴ Uncertainties represent one standard deviation. The spectrum is listed in Table S5 of the Supporting Information. ^bThe rotational constants were obtained in CCSD/cc-pVQZ calculations, whereas the centrifugal distortion constants were computed using the MP2/cc-pVTZ procedure. ^cRoot-mean-square deviation defined as $\text{rms}^2 = \Sigma[(\nu_{\text{obs}} - \nu_{\text{calc}})/u]^2/(N - P)$, where ν_{obs} and ν_{calc} are the observed and calculated frequencies, *u* is the uncertainty of the observed frequency, *N* is the number of transitions used in the least-squares fit, and *P* is the number of spectroscopic constants used in the fit. ^dNumber of transitions used in the fit.

Microwave Spectrum and Assignment of the Spectrum of *sc*. The MW spectrum was found to be of intermediate intensity and dense with absorption lines occurring every few MHz in the whole investigated spectral range. The theoretical predictions above indicate that *sc* is more stable than *ap* by 2–3 kJ/mol. *sc* has a statistical weight of 2 compared to a weight of 1 for *ap* because there are two mirror-image forms

Table 4. Stark Coefficients^a and Dipole Moment^a of the *sc* Conformer of C₃H₅CH₂F

transitions	M	Stark coefficients $\Delta E^{-2}/(10^{-6} \text{ MHz V}^{-2}) \text{ cm}^2$	
		obs	calc
3 _{0,3} ← 2 _{0,2}	1	−2.63(6) ^a	−2.61
4 _{1,4} ← 3 _{1,3}	0	−1.02(3)	−1.06
	1	1.39(2)	1.38
	2	8.92(15)	8.82
4 _{0,4} ← 3 _{0,3}	1	−0.761(9)	−0.767
	2	2.40(4)	2.38
	3	7.67(12)	7.63
4 _{1,3} ← 3 _{1,2}	1	−4.14(6)	−4.17
7 _{1,6} ← 7 _{0,7}	7	11.1(4)	11.3
8 _{1,7} ← 8 _{0,8}	8	8.65(15)	8.60
Dipole Moment ^b (10 ^{−30} C m)			
$\mu_a = 5.52(17)$ $\mu_b = 3.475(29)$ $\mu_c = 0.358139$ $\mu_{\text{TOT}} = 6.532(40)$			

^aUncertainties represent one standard deviation. ^bConversion factor: 1 D = 3.33564 × 10^{−30} C m. [$\mu_{\text{TOT}} = 1.958(12)$ D].

of *sc*. It was therefore immediately concluded that the majority of the strongest observed transitions must belong to *sc*. The high spectral density is consistent with both *ap* and *sc* having comparatively large dipole moment components along the *a*- and *b*-inertial axes (Table 1) according to the CCSD calculations above, as well as the fact that spectra of vibrationally excited states, particularly of *sc*, will contribute significantly to the spectrum because there are four fundamental vibrational normal modes below 500 cm^{−1} (Tables 2S of the Supporting Information).

sc has its major dipole-moment component along the *a*-inertial axis. Ray's asymmetry parameter⁵⁰ $\kappa \approx -0.94$ and pile-ups of *a*-type *R*-branch lines were therefore expected for this rotamer. The majority of the transitions of these pile-ups are modulated at relatively low Stark fields. The approximate frequencies of these "R-lines" were predicted using the CCSD rotational constants and the MP2 quartic centrifugal distortion constants shown in the last column of Table 2. Typical pile-ups,

Table 3. Spectroscopic Constants^a of Vibrationally Excited States of the *sc* Conformer of C₃H₅CH₂F

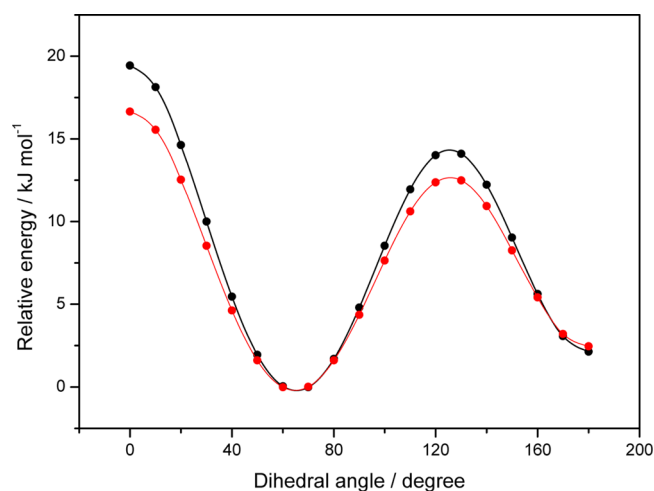
	first ex. tors.	second ex. tors.	third ex. tors.	fourth ex. tors.	fifth ex. tors.	sixth ex. tors.	lowest bend
<i>A</i> (MHz)	12700.7245(26)	12653.2666(43)	12608.5895(66)	12564.3915(74)	12518.560(16)	12474.80(11)	12745.2260(71)
<i>B</i> (MHz)	3178.81330(61)	3182.30140(80)	3186.0548(13)	3190.0765(16)	3194.4600(22)	3199.2486(85)	3176.7811(13)
<i>C</i> (MHz)	2862.39634(63)	2866.45126(80)	2870.5241(13)	2874.8420(16)	2879.5845(22)	2885.0769(87)	2859.0382(13)
<i>D_J</i> (kHz)	1.30911(56)	1.32776(80)	1.3737(24)	1.4233(29)	1.4931(42)	1.6442(66)	1.3016(24)
<i>D_{JK}</i> (kHz)	−4.6655(52)	−4.5483(63)	−4.3156(99)	−4.5422(79)	−5.203(15)	−6.077(17)	−5.453(12)
<i>D_K</i> (kHz)	257307(51)	24.793(34)	25.13(31)	26.67(18)	25.90(79)	26.344 ^b	25.40(29)
<i>d₁</i> (kHz)	−0.21838(14)	−0.22349(14)	−0.23167(20)	−0.24361(16)	−0.25839(32)	−0.21559 ^b	−0.21633(16)
<i>d₂</i> (kHz)	−0.012062(24)	−0.011879(46)	−0.012405(71)	−0.012788(68)	−0.01375(11)	−0.012105 ^b	−0.011179(55)
<i>H_J</i> (Hz)	0.00264(13)						
<i>H_{JK}</i> (Hz)	−0.0275(24)						
<i>H_{KJ}</i> (Hz)	0.0878(36)	0.118(42) ^c					
<i>H_K</i> (Hz)	−0.121(10)						
<i>h₁</i> (Hz)	0.000747(49) ^c						
rms ^d	1.239	1.246	1.340	1.396	1.348	1.129	1.343
<i>N</i> ^e	754	369	246	205	138	35	214

^aS-reduction *I*^r-representation.⁴⁴ Uncertainties represent one standard deviation. The spectra are found in the Supporting Information in Tables 6S–11S (successive excited states of the torsion) and in Table 12S (lowest bending vibration), ^bFixed; see text. ^cFurther sextic constants preset at zero in the least-squares fit. ^dRoot-mean-square deviation defined as $\text{rms}^2 = \Sigma[(\nu_{\text{obs}} - \nu_{\text{calc}})/u]^2/(N - P)$, where ν_{obs} and ν_{calc} are the observed and calculated frequencies, *u* is the uncertainty of the observed frequency, *N* is the number of transitions used in the least-squares fit, and *P* is the number of spectroscopic constants used in the fit. ^eNumber of transitions used in the fit.

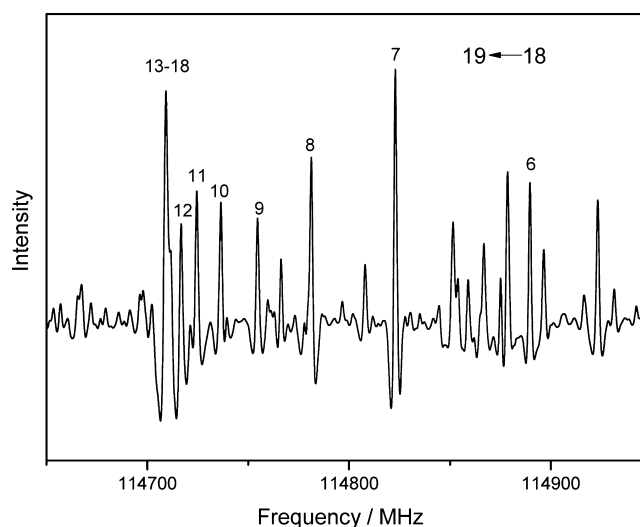
Table 5. Spectroscopic Constants of the Ground Vibrational State of the *ap* Conformer and Their Theoretical Counterparts

	ground state ^a	theory ^b
<i>A</i> (MHz)	9733.8910(86)	9851.02
<i>B</i> (MHz)	3814.6578(22)	3845.87
<i>C</i> (MHz)	3588.7808(22)	3619.23
Δ^c (10^{-20} u m ²)	−43.58106(5)	−43.07
<i>D_J</i> (kHz)	2.2950(57)	2.29
<i>D_{JK}</i> (kHz)	−0.6216(63)	−1.21
<i>D_K</i> (kHz)	4.75(40)	3.88
<i>d₁</i> (kHz)	−0.24772(11)	−0.255
<i>d₂</i> (kHz)	0.087294(48)	0.0735
<i>H_K</i> ^d (Hz)	20.5(64)	−0.162
rms ^e	1.274	
<i>N</i> ^f	293	

^aS-reduction *I*^r-representation.⁴⁴ Uncertainties represent one standard deviation. The spectrum is listed in Table 13S of the Supporting Information. ^bThe rotational constants were obtained in CCSD/cc-pVQZ calculations, whereas the centrifugal distortion constants were computed using the MP2/cc-pVTZ procedure. ^cDefined by $\Delta = I_c - I_a - I_b$, where *I_a*, *I_b*, and *I_c* are the principal moments of inertia. Conversion factor: $505379.05 \times 10^{-20}$ MHz u m². ^dFurther sextic constants preset at zero in the least-squares fit. ^eRoot-mean-square deviation defined as $\text{rms}^2 = \sum[(\nu_{\text{obs}} - \nu_{\text{calc}})/u]^2 / (N - P)$, where ν_{obs} and ν_{calc} are the observed and calculated frequencies, *u* is the uncertainty of the observed frequency, *N* is the number of transitions used in the least-squares fit, and *P* is the number of spectroscopic constants used in the fit. ^fNumber of transitions used in the fit.

**Figure 2.** MP2/cc-pVTZ (black curve) and B3LYP/cc-pVTZ (red curve) barriers to internal rotation about the H6C2–C9F12 bond.

an example of which is shown in Figure 3, were soon identified and readily assigned. The assignments were unambiguously confirmed using the RFMWDR technique.³³ The frequencies of the transitions assigned in this manner were weighted according to their estimated uncertainties and least-squares fitted to Watson's Hamiltonian using the S-reduction *I*^r-representation,⁴⁴ as implemented in Sørensen's program Rotfit.⁵¹ A set of preliminary spectroscopic constants were obtained in this manner and used to predict the approximate frequencies of *b*_Q-transitions, which are the strongest lines of the *b*-type variety. These transitions were found close to their predicted frequencies. The assignments were then gradually extended to include additional *a*- and *b*-type lines of higher and higher

**Figure 3.** A portion of the MW spectrum taken at a field strength of about 110 V/cm demonstrating the complexity of the spectrum. The intensity is in arbitrary units. This spectral region is dominated by absorption lines mainly associated with the *J* = 19 ← 18 *a*-type transitions of *sc*. Values of the *K*_{−1} pseudo quantum number are listed above several peaks belonging to the ground vibrational state. Lines with *K*_{−1} quantum numbers between 13 and 18 coalesce at a frequency of about 114710 MHz. Most of the remaining unlabeled transitions belong to vibrationally excited states of *sc*. Transitions with *K*_{−1} quantum numbers of 8 and 7 are more intense than expected due to overlap with other transitions.

values of the principal quantum number *J* and the pseudo-quantum number *K*_{−1}. Searches were also made for *c*-type lines, but none were found, presumably because of the small μ_c dipole moment (see below, Table 4). Ultimately, 1130 lines listed in Table 5S of the Supporting Information were assigned and used to determine the spectroscopic constants displayed in Table 2. The maximum value of *J* is 90, and *K*_{−1} has values up to 32. Transitions involving even higher values of *J* were searched for, but these lines were too weak to be assigned unambiguously. Their weakness is presumably due to an unfavorable Boltzmann factor. Sextic centrifugal distortion constants had to be employed in the fit in order to obtain a satisfactory dimensionless root-mean-square deviation of 1.274 (Table 2), whose definition is given in the footnote of Table 2.

The experimental rotational constants (Table 2) are smaller than the CCSD rotational constants (same table). The differences are −155.47, −23.03, and −22.55 MHz for *A*, *B*, and *C*, respectively, close to the MP2 values −122.56, −27.09, and −25.88 MHz obtained for the differences between the ground-state and equilibrium rotational constants (see Table 2S, Supporting Information). The fact that most of the difference between the CCSD and experimental rotational constants can be attributed to vibrations indicates that the CCSD structure is indeed very close to the equilibrium structure. This is expected for a compound composed of elements of the first and second row of the periodic table.

The experimental quartic centrifugal distortion constants (Table 2) deviate relatively more from their MP2 counterparts than the rotational constants do. The smallest relative deviation is found for *D_J* (1.5% deviation), while the largest deviation is seen for *d₂* (6.6%). The accuracy of the experimental sextic centrifugal distortion constants varies much. Their one standard deviation fluctuates from 2.6% (*H_{KJ}*) to 48% (*h₂*), and there is poor overall agreement with their MP2 equivalents.

Vibrationally Excited States of sc. The ground-state transitions were accompanied by a series of weaker lines with very similar Stark effects and RFMWDR patterns. These series were assumed to belong to the spectra of vibrationally excited states. The spectra of seven excited states belonging to two different vibrational modes were assigned in a manner analogous to that described for the ground vibrational state. Six of these excited states are assumed to belong to successively excited states of the torsion of the CH_2F group, and one excited state is considered to be the first excited state of the lowest bending vibration. The spectroscopic constants obtained from least-squares fits of the spectra of these excited states are shown in Table 3.

Five of the seven sextic centrifugal distortion constants were fitted for the first excited state of the torsion of the CH_2F group. The two remaining sextic constants h_2 and h_3 were preset at zero. Only one such constant, H_{Kp} , was fitted for the second excited state of this vibration, while only quartic constants were employed for the next three excited states. Only 35 transitions were assigned for the sixth excited state of the torsion, and only D_J and D_{JK} were fitted in this case. The remaining quartic constants were fixed at the ground-state values in the least-squares fit.

The four lowest normal modes of the *sc* conformer have anharmonic frequencies of 115, 238, 345, and 478 cm^{-1} , according to the MP2 calculations (Table 2S of the Supporting Information). The spectrum of the most intense excited state (Table 6S, Supporting Information) has an intensity of roughly 60% of that of the ground vibrational state at room temperature. Relative intensity measurements performed largely as described by Esbitt and Wilson⁵² yielded 112(20) cm^{-1} for this mode, which is assumed to be the first excited state of the torsion about the C2–C9 bond, whose MP2 anharmonic frequency is 115 cm^{-1} .

It is possible to compare the experimental and theoretical vibration–rotation constants defined by $\alpha_x = X_0 - X_{\text{ex}}$,⁴⁵ where X_0 is a rotational constants of the ground state and X_{ex} is a corresponding rotational constant of the excited state under consideration. The experimental vibration–rotation constants derived from the entries for the ground state (Table 2) and the first excited state of the torsion (Table 3) are $\alpha_A = 45.2101(32)$, $\alpha_B = -3.41302(79)$, and $\alpha_C = -4.04726(82)$ MHz, compared to the MP2 values of 40.78, -1.45 , and -2.68 MHz, respectively (Table 2S, Supporting Information). The agreement is satisfactory given the approximate nature of the MP2 calculations.

It is seen from Table 3 that the rotational constants of the six successively excited states of the torsion change in a regular fashion, which is typical for an essentially harmonic vibration.⁵³ This is illustrated in Figure 4.

An excited-state spectrum (Table 12S, Supporting Information) assumed to belong to the first excited state of the lowest bending vibration was also assigned, and its frequency was determined to be 265(30) cm^{-1} by relative intensity measurements, compared to the MP2 anharmonic frequency which is 238 cm^{-1} (Table 2S, Supporting Information). The vibration–rotation constants derived for this mode from Tables 2 and 3 are $\alpha_A = -0.7086(73)$, $\alpha_B = -1.3308(14)$, and $\alpha_C = -0.6891(14)$ MHz, in poor agreement with the MP2 values of -52.76 , -1.74 , and 1.18 MHz, respectively (Table 2S, Supporting Information). Obviously, quantum calculations at a higher methodological level than MP2/cc-pVTZ are needed

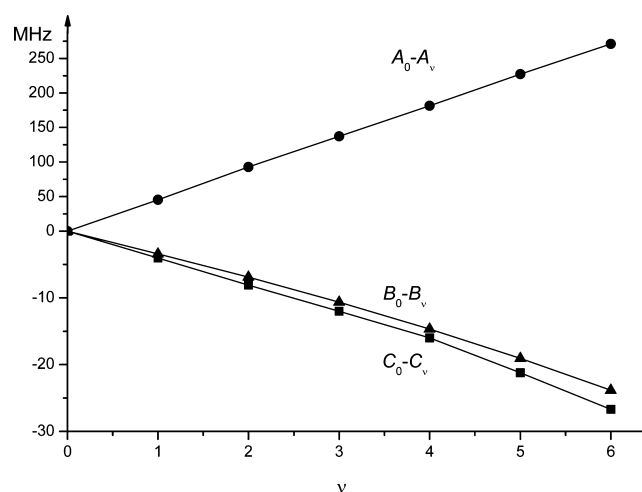


Figure 4. Variation of the rotational constants upon excitation of the CH_2F torsional vibration. Note the different scales of the positive and negative Y-axis.

to reproduce the vibration–rotation constants of this compound.

Dipole Moment of sc. The dipole moment was determined by least-squares fitting the second-order Stark coefficient shown in Table 4. The weight of each Stark coefficient was taken to be the inverse square of its standard deviation, which is also shown in the same table. The theoretical values of the second-order Stark coefficients were calculated as described by Golden and Wilson⁵⁴ using the program MB04.⁵⁵ The experimental dipole moment components are $\mu_a = 5.520(17)$, $\mu_b = 3.475(29)$, $\mu_c = 0.35(13)$, and $\mu_{\text{tot}} = 6.532(40) \times 10^{-30}$ C m [$1.958(12)$ D], where the uncertainties represent one standard deviation. The experimental values are in very good agreement with the calculated dipole moments at the CCSD/cc-pVQZ level of theory (5.56 , 3.42 , 0.48 , and 6.54×10^{-30} C m, respectively; Table 1).

Assignment of the Ground-State Spectrum of ap. This conformer has its major dipole moment component along the *b*-inertial axis according to the CCSD calculations (Table 1). Searches were therefore first made for its many ^bQ -transitions predicted to be comparatively strong. The $K_{-1} = 2 \leftarrow 1$ Q-branch series was first searched for and readily assigned for a spectrum that was significantly less strong than that of *sc*. Extension of the assignments to further ^bQ -series was straightforward and ultimately included a maximum value of $J = 48$. Strong *b*-type R-branch transitions are much fewer. The strongest ones comprise the $K_{-1} = 0 \leftarrow 1$ and $K_{-1} = 1 \leftarrow 0$ series. These transitions were found using a trial-and-error procedure. Finally, many “R-branch transitions with $J \geq 9$ were identified by their Stark-modulation patterns and fit to Watson’s Hamiltonian.⁴⁴ A total of 293 transitions (Table 13S, Supporting Information) were used to determine the spectroscopic constants shown in Table 5. The dipole moment could not be determined because relevant transitions had insufficient intensities to allow a quantitative determination of their Stark effects.

It is seen from Table 5 that the experimental rotational constants of the ground state are smaller than their CCSD equilibrium counterparts, just as in the case of *sc* (see above). The deviations are not large, -117.13 MHz for A , -31.22 MHz for B , and -30.45 MHz for C . The MP2 $B_0 - B_e$ differences are -77.71 , -49.11 , and -41.47 MHz, respectively (Table 1S, Supporting Information). This is taken as an indication that the

CCSD structure of **ap** is also very close to the equilibrium structure.

The fact that **ap** has a symmetry plane makes it meaningful to compare values of Δ defined by $\Delta = I_c - I_a - I_b$, where I_a , I_b , and I_c are the principal moments of inertia for similar compounds. A value of $-43.58106(5) \times 10^{-20} \text{ u m}^2$ shown in Table 5 is compared to the CCSD value ($-43.07 \times 10^{-20} \text{ u m}^2$). The difference of about $0.5 \times 10^{-20} \text{ u m}^2$ could be due largely to the CH_2F torsion. For comparison, the value of Δ in the anti-periplanar conformer of $\text{C}_3\text{H}_5\text{CH}_2\text{Cl}$ calculated from the reported rotational constants⁵⁶ is $-43.38 \times 10^{-20} \text{ u m}^2$.

The MP2 quartic centrifugal distortion constants are very similar to the experimental ones in the cases of D_J and d_1 , as seen in Table 5. The theoretical value of D_{JK} is almost twice as large as the experimental result, while D_K is off by 18% and d_2 deviates by 16% relative to the experimental counterparts. Obviously, more sophisticated quantum approaches are needed to improve agreement between theory and experiment in this case, but this was not possible with the computational resources available for us.

Energy Difference between **ap and **sc**.** The internal energy difference between these two forms was obtained from comparison of the intensities of several selected transitions of the ground states of the two conformers using the procedure outlined by Esbitt and Wilson.⁵² The dipole moment must be known in order to derive the energy difference. The experimental dipole moment of **ap** is not available. The CCSD dipole moments (Table 1) of the two forms were therefore used. The result was $E_{\text{ap}} - E_{\text{sc}} = 1.7 \text{ kJ/mol}$ with an estimated one standard deviation of 0.8 kJ/mol . This value is lower than $3.13(31) \text{ kJ/mol}$ found for this compound dissolved in xenon,^{1,4} demonstrating that even the apolar solvent xenon influences conformational composition. It is noted that the experimental value of $1.7(8) \text{ kJ/mol}$ is lower than the CCSD electronic energy difference (2.94 kJ/mol ; Table 1), the B3LYP electronic energy difference (2.65 kJ/mol), and the MP2 result corrected for zero-point energies (2.54 kJ/mol ; see above).

DISCUSSION

The energy difference between **sc** and **ap** has been derived by various experimental and theoretical methods. The results are summarized in Table 6. It is seen from this table that all methods but molecular mechanics predict **sc** to be the

Table 6. Experimental and Theoretical Determinations of Energy Differences between the **sc and **ap** Conformers of (Fluoromethyl)cyclopropane**

$E_{\text{ap}} - E_{\text{sc}}$	method	phase	reference
−2.2	molecular mechanics	gas	2
0.8	MP4(SDQ)/6-311G**	gas	3
2.99(30)	variable temperature ^a	xenon solution	4
3.13(31)	variable temperature ^a	xenon solution	1
3.88	MP2/6-311G(2df,2pd)	gas	1
4.21	B3LYP/6-311G(2df,2pd)	gas	1
1.7(8)	microwave	gas	58
2.94	CCSD/cc-pVQZ	gas	58
2.65	MP2/cc-pVTZ	gas	58
2.54	B3LYP/cc-pVTZ	gas	58

^aThe energy difference has been obtained by measuring the variation of the intensities of spectral bands with temperature with (fluoromethyl)cyclopropane dissolved in a xenon liquid solution.

lower-energy conformer by 1–4 kJ/mol. The present experimental gas-phase energy difference is somewhat smaller than most of the other results.

There are probably several reasons why the **sc** conformer of (fluoromethyl)cyclopropane is $1.7(8) \text{ kJ/mol}$ more stable than **ap**. Several relative short nonbonded contacts exist in **ap**. The CCSD nonbonded distance between the fluorine atom F12 (Figure 1) and the hydrogen atoms H5 and H7 is 255 pm (Table 3S of the Supporting Information) compared to the sum, 246 pm , of the van der Waals radii of fluorine (140 pm)⁵⁷ and hydrogen (106 pm).⁵⁷ This interaction is therefore not strong but presumably stabilizing **ap** due to the electronegative character of fluorine and the electropositive nature of hydrogen. Steric crowding due to the close proximity of the fluorine atom and electrons of the cyclopropyl ring is another effect that could destabilize **ap** relative to **sc**. The latter conformer should profit from the *gauche* effect,²⁸ which predicts that electronegative substituents prefer synclinal conformations. The fact that the H6–C2–C9–F12 dihedral is 65.0° (Table 4S, Supporting Information) and not 60° in **sc** is harder to explain but could be due to a slight repulsion between H7 and H11 and a minor attraction between the fluorine atom and H5. The observed energy difference of $E_{\text{ap}} - E_{\text{sc}} = 1.7(8) \text{ kJ/mol}$ must therefore obviously be a compromise of several intramolecular forces.

The **ap** – **sc** energy differences have been investigated for the other three halogen-substituted methylcyclopropane derivatives. In gaseous $\text{C}_3\text{H}_5\text{CH}_2\text{Cl}$, the enthalpy difference is $3.3(13) \text{ kJ/mol}$.⁶ In xenon solution, an enthalpy difference of $3.28(25) \text{ kJ/mol}$ was obtained.⁸ $\Delta H = 4.58(35) \text{ kJ/mol}$ was determined for $\text{C}_3\text{H}_5\text{CH}_2\text{Br}$ in the same solvent.⁸ Wurrey et al.¹⁰ concluded that $\text{C}_3\text{H}_5\text{CH}_2\text{I}$ exists solely in the synclinal conformation in all states of matter. The present study is therefore in accord with the general view that the synclinal conformers of halogen-substituted methylcyclopropanes become increasingly more stable as the size of the halogen increases. Steric crowding appears to be a predominating cause of this behavior.

ASSOCIATED CONTENT

Supporting Information

Preparation of the title compound. Results of the theoretical calculations, including electronic energies, molecular structures, dipole moments, harmonic and anharmonic vibrational frequencies, rotational and centrifugal distortion constants, and rotation–vibration constants. Microwave spectra of the ground and vibrationally excited states. This material is available free of charge via the Internet at <http://pubs.acs.org>.

AUTHOR INFORMATION

Corresponding Author

*Phone: +47 2285 5674. Fax: +47 2285 5441. E-mail: harald.mollendal@kjemi.uio.no.

Notes

The authors declare no competing financial interest.

ACKNOWLEDGMENTS

We thank Anne Horn for her skillful assistance. This work has been supported by the Research Council of Norway through a Centre of Excellence Grant (Grant No. 179568/V30). It has also received support from the Norwegian Supercomputing Program (NOTUR) through a grant of computer time

(Grant No. NN4654K). J.-C.G. thanks the Centre National d'Etudes Spatiales (CNES) for financial support.

REFERENCES

- (1) Durig, J. R.; Yu, Z.; Zheng, C.; Guirgis, G. A. Conformational Studies of Fluoromethylcyclopropane from Temperature-Dependent FT-IR Spectra of Xenon Solutions and Ab Initio Calculations. *J. Phys. Chem. A* **2004**, *108*, 5353–5364.
- (2) Stølevik, R.; Bakken, P. Conformational Analysis of the Halomethyl Cyclopropanes and the Halosilyl Cyclopropanes by Molecular Mechanics Calculations. *J. Mol. Struct.* **1989**, *196*, 285–289.
- (3) Saebo, S.; Kavana, K. Molecular Structure and Conformation of Fluoromethyl-substituted Cyclopropane and Oxirane. MP4(SDQ)/6-311G** results. *J. Mol. Struct.: THEOCHEM* **1991**, *81*, 447–457.
- (4) Durig, J. R.; Yu, Z.; Shen, S.; Warren, R.; Verma, V. N.; Guirgis, G. A. Conformational Studies of Monosubstituted Three-membered Rings by Variable Temperature FT-IR Spectra of Rare Gas Solutions. *J. Mol. Struct.* **2001**, *563–564*, 141–145.
- (5) Heineking, N.; Grabow, J. U.; Merke, I. Molecular Beam Fourier Transform Microwave Spectra of (Chloromethyl)cyclopropane and (Chloromethyl)oxirane. *J. Mol. Struct.* **2002**, *612*, 231–244.
- (6) Durig, J. R.; Godbey, S. E.; Faust, S. A. Far Infrared and Low Frequency Raman Spectra and Conformational Stability of Gaseous (Chloromethyl)cyclopropane and (Bromomethyl)cyclopropane. *J. Mol. Struct.* **1988**, *176*, 123–135.
- (7) Schei, S. H. (Chloromethyl)cyclopropane. Molecular Structure and Conformation in the Gas Phase as Determined by Electron Diffraction and Compared to Molecular Mechanics Calculation. *Acta Chem. Scand., Ser. A* **1983**, *A37*, 15–23.
- (8) Durig, J. R.; Shen, S.; Zhu, X.; Wurrey, C. J. Conformational and Structural Studies of Chloromethylcyclopropane and Bromomethylcyclopropane from Temperature Dependent FT-IR Spectra of Xenon Solutions and Ab Initio Calculations. *J. Mol. Struct.* **1999**, *485–486*, 501–521.
- (9) Wurrey, C. J.; Krishnamoorthi, R.; Pechsiri, S.; Kalasinsky, V. F. Vibrational Spectra and Conformations of (Bromomethyl)cyclopropane and Epibromohydrin. *J. Raman Spectrosc.* **1982**, *12*, 95–101.
- (10) Wurrey, C. J.; Yeh, Y. Y.; Krishnamoorthi, R.; Berry, R. J.; DeWitt, J. E.; Kalasinsky, V. F. Vibrational Spectra and Conformations of (Iodomethyl)Cyclopropane and Epiiodohydrin. *J. Phys. Chem.* **1984**, *88*, 4059–4063.
- (11) Newby, J. J.; Peebles, R. A.; Peebles, S. A. Heavy Atom Structure and Conformer Stabilities of Cyclopropyl Carbinol from Rotational Spectroscopy and Ab Initio Calculations. *J. Mol. Struct.* **2005**, *740*, 133–142.
- (12) Marstokk, K.-M.; Møllendal, H. A Microwave and Ab Initio Study of the Conformational Properties and Intramolecular Hydrogen Bonding of Cyclopropanemethanethiol. *Acta Chem. Scand.* **1991**, *45*, 354–360.
- (13) Cole, G. C.; Møllendal, H.; Guillemin, J.-C. Spectroscopic and Quantum Chemical Study of the Novel Compound Cyclopropylmethylselenol. *J. Phys. Chem. A* **2006**, *110*, 2134–2138.
- (14) Marstokk, K. M.; Møllendal, H. Microwave Spectrum, Conformational Equilibrium, Intramolecular Hydrogen Bonding, Dipole Moments, Nitrogen-14 Nuclear Quadrupole Coupling Constants and Centrifugal Distortion Constants of (Aminomethyl)cyclopropane. *Acta Chem. Scand., Ser. A* **1984**, *A38*, 387–398.
- (15) Cole, G. C.; Møllendal, H.; Guillemin, J.-C. Spectroscopic and Quantum Chemical Study of Cyclopropylmethylphosphine, a Candidate for Intramolecular Hydrogen Bonding. *J. Phys. Chem. A* **2005**, *109*, 7134–7139.
- (16) Wurrey, C. J.; Shen, S.; Goune, T. K.; Durig, J. R. Conformational Stability of Ethylcyclopropane from Raman Spectra, Temperature Dependent FT-IR Spectra of Xenon Solutions and Ab Initio Calculations. *J. Mol. Struct.* **1997**, *406*, 207–218.
- (17) Durig, J. R.; Little, T. S.; Zhu, X.; Dakkouri, M. Vibrational Spectra and Assignments, Conformational Stability, and Ab Initio Calculations of Cyclopropylmethylsilanes. *J. Mol. Struct.* **1993**, *293*, 15–18.
- (18) Foellmer, M. D.; Murray, J. M.; Serafin, M. M.; Steber, A. L.; Peebles, R. A.; Peebles, S. A.; Eichenberger, J. L.; Guirgis, G. A.; Wurrey, C. J.; Durig, J. R. Microwave Spectra and Barrier to Internal Rotation in Cyclopropylmethylsilane. *J. Phys. Chem. A* **2009**, *113*, 6077–6082.
- (19) Little, T. S.; Zhu, X.; Wang, A.; Durig, J. R. Spectra and Structure of Small Ring Compounds-LXI. IR and Raman Spectra, Vibrational Assignment, Conformational Stability and Ab Initio Calculations of Cyclopropylmethylsilane. *Spectrochim. Acta, Part A* **1993**, *49A*, 1913–1933.
- (20) Dakkouri, M.; Hermann, T. A Combined Ab Initio and Gas-Phase Electron Diffraction Investigation of the Molecular Structure and Conformation of (Silylmethyl)cyclopropane. *J. Mol. Struct.* **1995**, *346*, 239–248.
- (21) Little, T. S.; Vaughn, C. A.; Zhu, X.; Dakkouri, M.; Durig, J. R. Spectra and Structure of Small-Ring Compounds. LXII. Raman and Infrared Spectra, Conformational Stability, Vibrational Assignment and Ab Initio Calculations of Cyclopropylmethyltrifluorosilane. *J. Raman Spectrosc.* **1994**, *25*, 735–746.
- (22) Dakkouri, M. The Molecular Structure and Conformation of (Trifluorosilylmethyl)cyclopropane as Determined by Gas-Phase Electron Diffraction and Ab Initio Calculations. *J. Mol. Struct.* **1997**, *413–414*, 133–152.
- (23) Su, C. F.; Cook, R. L.; Wurrey, C. J.; Kalasinsky, V. F. Microwave Spectrum of (Cyanomethyl)cyclopropane. *J. Mol. Spectrosc.* **1986**, *118*, 277–287.
- (24) Wurrey, C. J.; Yeh, Y. Y.; Weakley, M. D.; Kalasinsky, V. F. Vibrational Spectra and Conformational Behavior of (Cyanomethyl)cyclopropane. *J. Raman Spectrosc.* **1984**, *15*, 179–185.
- (25) Caminati, W.; Danieli, R.; Dakkouri, M.; Bitschenauer, R. Conformational Equilibrium in (Cyclopropylmethyl)acetylene: a Microwave Spectroscopy and ab Initio Calculation Study. *J. Phys. Chem.* **1995**, *99*, 1867–1872.
- (26) Dakkouri, M.; Typke, V. Structural and Conformational Analysis of the Isoelectronic Isovalent Molecules: (Ethynylmethyl)cyclopropane and Ethynylcyclobutane. A Combined Electron Diffraction, Rotational Constants and Ab Initio Study. *J. Mol. Struct.* **2000**, *550–551*, 349–364.
- (27) Samdal, S.; Møllendal, H.; Guillemin, J.-C. Microwave Spectrum, Conformational Properties, and Dipole Moment of Cyclopropylmethyl Isocyanide ($C_3H_5CH_2NC$). *J. Phys. Chem. A* **2013**, *117*, 5073–5081.
- (28) Wolfe, S. Gauche effect. Stereochemical Consequences of Adjacent Electron Pairs and Polar Bonds. *Acc. Chem. Res.* **1972**, *5*, 102–111.
- (29) Walsh, A. D. Structures of Ethylene Oxide, Cyclopropane, and Related Molecules. *Trans. Faraday Soc.* **1949**, *45*, 179–190.
- (30) Møllendal, H. Recent Gas-Phase Studies of Intramolecular Hydrogen Bonding. *NATO ASI Ser., Ser. C* **1993**, *410*, 277–301.
- (31) Kraft, B. M.; Lachicotte, R. J.; Jones, W. D. Aliphatic and Aromatic Carbon-Fluorine Bond Activation with $Cp^*_2ZrH_2$: Mechanisms of Hydrodefluorination. *J. Am. Chem. Soc.* **2001**, *123*, 10973–10979.
- (32) Samdal, S.; Grønås, T.; Møllendal, H.; Guillemin, J. C. Microwave Spectrum and Conformational Properties of 4-Isocyanobutene. *J. Phys. Chem. A* **2014**, *118*, 1413–1419.
- (33) Wodarczyk, F. J.; Wilson, E. B., Jr. Radio Frequency-Microwave Double Resonance as a Tool in the Analysis of Microwave Spectra. *J. Mol. Spectrosc.* **1971**, *37*, 445–463.
- (34) Møllendal, H.; Leonov, A.; de Meijere, A. A Microwave and Quantum Chemical Study of the Conformational Properties and Intramolecular Hydrogen Bonding of 1-Fluorocyclopropanecarboxylic Acid. *J. Phys. Chem. A* **2005**, *109*, 6344–6350.
- (35) Möller, C.; Plesset, M. S. Note on the Approximation Treatment for Many-Electron Systems. *Phys. Rev.* **1934**, *46*, 618–622.

- (36) Cizek, J. Use of the Cluster Expansion and the Technique of Diagrams in Calculations of Correlation Effects in Atoms and Molecules. *Adv. Chem. Phys.* **1969**, *14*, 35–89.
- (37) Purvis, G. D., III; Bartlett, R. J. A Full Coupled-Cluster Singles and Doubles Model: The Inclusion of Disconnected Triples. *J. Chem. Phys.* **1982**, *76*, 1910–1918.
- (38) Scuseria, G. E.; Janssen, C. L.; Schaefer, H. F., III. An Efficient Reformulation of the Closed-Shell Coupled Cluster Single and Double Excitation (CCSD) Equations. *J. Chem. Phys.* **1988**, *89*, 7382–7387.
- (39) Scuseria, G. E.; Schaefer, H. F., III. Is Coupled Cluster Singles and Doubles (CCSD) More Computationally Intensive Than Quadratic Configuration Interaction (QCISD)? *J. Chem. Phys.* **1989**, *90*, 3700–3703.
- (40) Frisch, M. J.; Trucks, G. W.; Schlegel, H. B.; Scuseria, G. E.; Robb, M. A.; Cheeseman, J. R.; Scalmani, G.; Barone, V.; Mennucci, B.; Petersson, G. A.; et al. *Gaussian 09*, revision B.01; Gaussian, Inc: Wallingford, CT, 2010.
- (41) Werner, H.-J.; Knowles, P. J.; Knizia, G.; Manby, F. R.; Schütz, M.; et al. *MOLPRO*, version 2010.1, a Package of Ab Initio Programs; 2010; <http://www.molpro.net/>.
- (42) Lee, C.; Yang, W.; Parr, R. G. Development of the Colle-Salvetti Correlation-Energy Formula Into a Functional of the Electron Density. *Phys. Rev. B* **1988**, *37*, 785–789.
- (43) Peterson, K. A.; Dunning, T. H., Jr. Accurate Correlation Consistent Basis Sets for Molecular Core-Valence Correlation Effects: The Second Row Atoms Al–Ar, and the First Row Atoms B–Ne Revisited. *J. Chem. Phys.* **2002**, *117*, 10548–10560.
- (44) Watson, J. K. G. *Vibrational Spectra and Structure*; Elsevier: Amsterdam, The Netherlands, 1977; Vol. 6.
- (45) Gordy, W.; Cook, R. L. *Microwave Molecular Spectra. In Techniques of Chemistry*; John Wiley & Sons: New York, 1984; Vol. XVII.
- (46) McKean, D. C.; Craig, N. C.; Law, M. M. Scaled Quantum Chemical Force Fields for 1,1-Difluorocyclopropane and the Influence of Vibrational Anharmonicity. *J. Phys. Chem. A* **2008**, *112*, 6760–6771.
- (47) Endo, Y.; Chang, M. C.; Hirota, E. The Microwave Spectrum of Cyclopropane-1,1-d₂. Molecular Structure of Cyclopropane. *J. Mol. Spectrosc.* **1987**, *126*, 63–71.
- (48) Penn, R. E.; Boggs, J. E. Substituent-Induced Asymmetry of the Cyclopropane Ring. *J. Chem. Soc., Chem. Commun.* **1972**, 666–667.
- (49) Demaison, J.; Breidung, J.; Thiel, W.; Papoušek, D. The equilibrium Structure of Methyl Fluoride. *Struct. Chem.* **1999**, *10*, 129–133.
- (50) Ray, B. S. The Characteristic Values of an Asymmetric Top. *Z. Phys.* **1932**, *78*, 74–91.
- (51) Sørensen, G. O. Centrifugal Distortion Analysis of Asymmetric Top Molecules. The Microwave Spectrum of Pyridine. *J. Mol. Spectrosc.* **1967**, *22*, 325–346.
- (52) Esbitt, A. S.; Wilson, E. B. Relative Intensity. *Rev. Sci. Instrum.* **1963**, *34*, 901–907.
- (53) Herschbach, D. R.; Laurie, V. W. Influence of Vibrations on Molecular Structure Determinations. I. General Formulation of Vibration-Rotation Interactions. *J. Chem. Phys.* **1962**, *37*, 1668–1686.
- (54) Golden, S.; Wilson, E. B. The Stark Effect for a Rigid Asymmetric Rotor. *J. Chem. Phys.* **1948**, *16*, 669–685.
- (55) Marstokk, K.-M.; Møllendal, H. Computer Programs for the Asymmetric Rotor. *J. Mol. Struct.* **1969**, *4*, 470–472.
- (56) Fujiwara, F. G.; Chang, J. C.; Kim, H. Microwave Spectrum and Rotational Isomers of Cyclopropylcarbonyl Chloride and Epichlorohydrin. *J. Mol. Struct.* **1977**, *41*, 177–182.
- (57) Bondi, A. van der Waals Volumes and Radii. *J. Phys. Chem.* **1964**, *68*, 441–451.
- (58) This work.